

1N-34  
12663  
14P

# Dynamic and Thermal Turbulent Time Scale Modelling for Homogeneous Shear Flows

John R. Schwab  
*Lewis Research Center*  
*Cleveland, Ohio*

and

Budugur Lakshminarayana  
*Pennsylvania State University*  
*University Park, Pennsylvania*

Prepared for the  
Fluids Engineering Division Summer Meeting  
sponsored by the American Society of Mechanical Engineers  
Lake Tahoe, Nevada, June 19-23, 1994

(NASA-TM-106635) DYNAMIC AND  
THERMAL TURBULENT TIME SCALE  
MODELLING FOR HOMOGENEOUS SHEAR  
FLOWS (NASA. Lewis Research  
Center) 14 p

N94-35253

Unclas

G3/34 0012663



National Aeronautics and  
Space Administration



# DYNAMIC AND THERMAL TURBULENT TIME SCALE MODELLING FOR HOMOGENEOUS SHEAR FLOWS

**John R. Schwab**

Internal Fluid Mechanics Division  
NASA Lewis Research Center  
Cleveland, Ohio

**Budugur Lakshminarayana**

Department of Aerospace Engineering  
Pennsylvania State University  
University Park, Pennsylvania

## ABSTRACT

A new turbulence model, based upon dynamic and thermal turbulent time scale transport equations, is developed and applied to homogeneous shear flows with constant velocity and temperature gradients. The new model comprises transport equations for  $k$ , the turbulent kinetic energy;  $\tau$ , the dynamic time scale;  $k_\theta$ , the fluctuating temperature variance; and  $\tau_\theta$ , the thermal time scale. It offers conceptually parallel modelling of the dynamic and thermal turbulence at the two-equation level, and eliminates the customary prescription of an empirical turbulent Prandtl number,  $Pr_t$ , thus permitting a more generalized prediction capability for turbulent heat transfer in complex flows and geometries. The new model also incorporates constitutive relations, based upon invariant theory, that allow the effects of non-equilibrium to modify the primary coefficients for the turbulent shear stress and heat flux.

Predictions of the new model, along with those from two other similar models, are compared with experimental data for decaying homogeneous dynamic and thermal turbulence, homogeneous turbulence with constant temperature gradient, and homogeneous turbulence with constant temperature gradient and constant velocity gradient. The new model offers improvement in agreement with the data for most cases considered in this work, although it was no better than the other models for several cases where all the models performed poorly.

## NOMENCLATURE

A, B	nondimensional parameters
$c_1, c_2, c_3, c_4$	constants in $\epsilon_\theta$ equation
$c_A, c_B$	constants in $c_\lambda$ equation
$c_{\epsilon 1}, c_{\epsilon 2}$	constants in $\epsilon$ equation
$c_\lambda$	primary coefficient in $\langle v\theta \rangle$ equation
$c_\mu$	primary coefficient in $\langle uv \rangle$ equation
$c_{\tau 1}, c_{\tau 2}$	constants in $\tau$ equation

$c_{\tau\theta 1}, c_{\tau\theta 2}, c_{\tau\theta 3}, c_{\tau\theta 3}$	constants in $\tau_\theta$ equation
$h$	total channel height
$k$	turbulent kinetic energy, $\langle uu + vv + ww \rangle / 2$
$k_\theta$	fluctuating temperature variance, $\langle \theta\theta \rangle / 2$
$M$	grid spacing
$P_k$	production of $k$ , $-\langle uv \rangle dU/dy$
$P_{k\theta}$	production of $k_\theta$ , $-\langle v\theta \rangle d\Theta/dy$
$Pr_t$	turbulent Prandtl number
$R$	time scale ratio, $\tau_\theta / \tau$
$u, v, w$	fluctuating velocity components in x, y and z directions
$U$	mean velocity in x direction
$x, y, z$	streamwise and transverse coordinates
$\epsilon$	dissipation rate of $k$
$\epsilon_\theta$	dissipation rate of $k_\theta$
$\tau$	dynamic time scale, $k / \epsilon$
$\tau_\theta$	thermal time scale, $k_\theta / \epsilon_\theta$
$\theta$	fluctuating temperature
$\Theta$	mean temperature
*	normalized value
$\langle \rangle$	averaged value

## INTRODUCTION

Modelling of the temperature field in turbulent flows is relatively inferior to modelling of the velocity field. The most popular methods merely use a constant Prandtl number,  $Pr_t$ , to infer the turbulent thermal diffusivity from a turbulent viscosity computed by a two-equation model or an algebraic model. Even in simple flows,  $Pr_t$  is not a universal constant (Reynolds, 1975), and can exhibit substantial variation near a wall (Antonia and Kim, 1991;

Bagheri, Strataridakis, and White, 1992). Transport models for the turbulent heat fluxes have been developed (Shih and Lumley, 1986; Jones and Musonge, 1988; Lai and So, 1990), but they suffer from complexities and uncertainties similar to those hindering the development and application of transport models for the turbulent stresses.

Two-equation models for the turbulent thermal diffusivity have been developed (Youssef, Nagano, and Tagawa, 1992; Sommer, So, and Zhang, 1993b; Shabbir, 1994) to offer conceptually parallel modelling of the dynamic and thermal turbulence, and elimination of the prescription of  $Pr_t$ . These approaches permit relatively economical, generalized prediction of turbulent temperature fields in complex flows and geometries. They employ transport equations for  $k$ , the turbulent kinetic energy;  $\epsilon$ , the dissipation rate of  $k$ ;  $k_\theta$ , the fluctuating temperature variance; and  $\epsilon_\theta$ , the dissipation rate of  $k_\theta$ . In this work, we develop two-equation models that employ transport equations for  $\tau$ , the dynamic turbulent time scale, and  $\tau_\theta$ , the thermal turbulent time scale, to replace those for  $\epsilon$  and  $\epsilon_\theta$ .

The traditional choice of the respective dissipation rates,  $\epsilon$  and  $\epsilon_\theta$ , as the second dependent variables, suffers due to the lack of simple, economical boundary conditions. Both dissipation rates asymptote to non-zero values at the wall. Exact values can be determined from the degenerate form of the  $k$  and  $k_\theta$  equations at the wall, but this involves the computation of the second derivatives of  $k$  and  $k_\theta$ , and may cause problems due to excessive stiffness and additional coupling of the first and second equations in each model.

Our choice of the turbulent time scales as dependent variables allows much simpler zero-valued boundary conditions at a solid wall. Since  $\tau = k / \epsilon$ , and  $k$  vanishes at the wall, we can apply the same boundary condition for  $\tau$ . Sommer, So, and Zhang (1993a) have shown that the assumption of vanishing temperature fluctuations at the wall is very reasonable, even for specified heat-flux boundary conditions. Since  $\tau_\theta = k_\theta / \epsilon_\theta$ , we can apply the same assumption for the  $\tau_\theta$  boundary condition.

The dynamic  $k$ - $\tau$  model is essentially identical to that developed earlier by Speziale, Abid, and Anderson (1992) through direct transformation of the  $k$ - $\epsilon$  equations using the definition  $\tau = k / \epsilon$ . Our thermal  $k_\theta$ - $\tau_\theta$  model is developed along similar lines through direct transformation of the  $k_\theta$ - $\epsilon_\theta$  equations using the definition  $\tau_\theta = k_\theta / \epsilon_\theta$ . Both models also incorporate constitutive relations, based upon invariant theory (Shih and Lumley, 1993), that allow the effects of non-equilibrium to modify the primary coefficients for the turbulent shear stress and heat flux.

Although one of the primary benefits of our new model results from the simpler boundary conditions to be specified at a wall, it is prudent to initially validate any new model by comparison with experimental data for simpler homogeneous shear flows. In this work, we compare the predictions of our new model with the predictions of the models of Youssef, Nagano, and Tagawa (1992), designated YNT, and Sommer, So, and Zhang (1993b), designated SSZ, with experimental data for decaying homogeneous dynamic and thermal turbulence (Warhaft and Lumley, 1978); homogeneous turbulence with constant temperature gradient (Sirivat and Warhaft, 1983); and homogeneous turbulence with constant temperature gradient and constant velocity gradient (Tavoularis and

Corrsin, 1981).

In all of these flows, the combination of transverse homogeneity of the turbulent correlations and streamwise homogeneity of the mean velocity and temperature uncouples the turbulent transport equations from the mean transport equations. The homogeneity also causes all diffusion terms to vanish, and reduces the turbulent transport equations to ordinary differential equations. This greatly simplifies the transport equations, and is the primary attraction of using homogeneous shear flows for validation of turbulence models.

## DEVELOPMENT OF THE DYNAMIC MODEL

For the simple homogeneous flows considered in this work, the standard transport equations for  $k$  and  $\epsilon$  can be written as:

$$U \frac{dk}{dx} = -\langle uv \rangle \frac{dU}{dy} - \epsilon = P_k - \epsilon \quad (1)$$

$$U \frac{d\epsilon}{dx} = c_{\epsilon 1} \frac{\epsilon}{k} P_k - c_{\epsilon 2} \frac{\epsilon^2}{k} \quad (2)$$

We note that equation (1) is an exact equation, while equation (2) is a generally-accepted modelled equation.

Using the definition  $\tau = k / \epsilon$ , we construct a similar transport equation for  $\tau$  (Speziale, Abid, and Anderson, 1992):

$$U \frac{d\tau}{dx} = -c_{\tau 1} \frac{\tau}{k} P_k + c_{\tau 2} \quad (3)$$

where  $c_{\tau 1} = c_{\epsilon 1} - 1 = 0.44$  and  $c_{\tau 2} = c_{\epsilon 2} - 1 = 0.8$ . We note that the first term on the right-hand side, representing the transformed production terms, is now negative, given the definition of  $\langle uv \rangle$ , while the second term, representing the transformed dissipation terms, is now positive.

Shih, Zhu, and Lumley (1993) derived an algebraic Reynolds stress model using invariant theory and realizability constraints. For the simple homogeneous flows considered in this work, we adopt the linear form of their constitutive equation for the shear stress:

$$-\langle uv \rangle = c_\mu k \tau \frac{dU}{dy} \quad (4)$$

The primary coefficient,  $c_\mu$ , was determined to be a function of the nondimensional parameter  $A$ :

$$c_\mu = \frac{2/3}{(1.25 + 1.9A)} \quad (5)$$

$$A = \frac{k}{\epsilon} \left\| \frac{dU}{dy} \right\| = \tau \left\| \frac{dU}{dy} \right\| = \sqrt{\frac{k\tau}{\epsilon}} \left\| \frac{dU}{dy} \right\| \quad (6)$$

The parameter  $A$  is proportional to the square root of the ratio of production to dissipation, thus allowing  $c_\mu$  to vary from its cus-

tomy constant value of 0.09, as determined from equilibrium and constant-stress assumptions in the log-law region of a boundary layer. In this region,  $A = 3.3$ , leading to  $c_\mu = 0.088$ .

## DEVELOPMENT OF THE THERMAL MODEL

For the simple homogeneous flows considered in this work, the standard transport equations for  $k_\theta$  and  $\varepsilon_\theta$  can be written as:

$$U \frac{dk_\theta}{dx} = -\langle v\theta \rangle \frac{d\Theta}{dy} - \varepsilon_\theta = P_{k\theta} - \varepsilon_\theta \quad (7)$$

$$U \frac{d\varepsilon_\theta}{dx} = c_1 \frac{\varepsilon_\theta}{k_\theta} P_{k\theta} + c_2 \frac{\varepsilon_\theta}{k} P_k - c_3 \frac{\varepsilon_\theta^2}{k_\theta} - c_4 \frac{\varepsilon \varepsilon_\theta}{k} \quad (8)$$

We note that equation (7) is an exact equation, while equation (8) is a modelled equation, first suggested by Newman, Launder, and Lumley (1981), and later modified by Nagano and Kim (1988), to include the second production term.

Using the definition  $\tau_\theta = k_\theta / \varepsilon_\theta$ , we construct a similar transport equation for  $\tau_\theta$ :

$$U \frac{d\tau_\theta}{dx} = c_{\tau\theta 1} \frac{\tau_\theta}{k_\theta} P_{k\theta} + c_{\tau\theta 2} \frac{\tau_\theta}{k} P_k + c_{\tau\theta 3} \frac{\tau_\theta}{\tau} + c_{\tau\theta 4} \quad (9)$$

The constants  $c_{\tau\theta 1}$ ,  $c_{\tau\theta 2}$ ,  $c_{\tau\theta 3}$ , and  $c_{\tau\theta 4}$  could be determined from  $c_1$ ,  $c_2$ ,  $c_3$ , and  $c_4$  in the  $\varepsilon_\theta$  transport equation. However, since the values for these constants in the  $\varepsilon_\theta$  transport equation are not as well-tested as those in the standard  $\varepsilon$  transport equation, we shall directly determine values for  $c_{\tau\theta 1}$ ,  $c_{\tau\theta 2}$ ,  $c_{\tau\theta 3}$ , and  $c_{\tau\theta 4}$  by considering the behavior of the time scale ratio,  $R = \tau_\theta / \tau$ , in various homogeneous shear flow experiments.

The new model requires a constitutive equation for the turbulent heat flux. The YNT model uses the following relation:

$$-\langle v\theta \rangle = c_\lambda \frac{k^2}{\varepsilon} [2R] \frac{d\Theta}{dy} \quad (10)$$

while the SSZ model uses:

$$-\langle v\theta \rangle = c_\lambda \frac{k^2}{\varepsilon} \sqrt{2R} \frac{d\Theta}{dy} \quad (11)$$

In both models,  $R = \tau_\theta / \tau$ , and  $c_\lambda$  is constant and equal to 0.1. Both models are obviously equivalent when  $R$  attains its equilibrium value of 0.5, as determined by Beguier, Dekeyser, and Launder (1978).

Shih and Lumley (1993) proposed a constitutive equation, based upon invariant theory, for the turbulent heat flux. For the simple homogeneous flows in this work, its first term reduces to a form equivalent to that employed by the SSZ model, although  $c_\lambda$  is now allowed to be a function of the invariants:

$$-\langle v\theta \rangle = c_\lambda \frac{k^2}{\varepsilon} \sqrt{2R} \frac{d\Theta}{dy} \quad (12)$$

They derived the above form using the nondimensional parameters  $A$ ,  $R$ , and  $B$ , where  $B$  is given by:

$$B = \frac{k}{\sqrt{\varepsilon \varepsilon_\theta}} \left\| \frac{d\Theta}{dy} \right\| \quad (13)$$

We propose an alternative form for  $B$  that will be proportional to the square root of the ratio of thermal production to thermal dissipation, similar to  $A$ :

$$B = \sqrt{\frac{k \tau_\theta}{\varepsilon_\theta}} \left\| \frac{d\Theta}{dy} \right\| = \tau_\theta \sqrt{\frac{k}{k_\theta}} \left\| \frac{d\Theta}{dy} \right\| \quad (14)$$

Using this form, we obtain the following constitutive equation for the turbulent heat flux:

$$-\langle v\theta \rangle = c_\lambda k \tau_\theta \frac{d\Theta}{dy} \quad (15)$$

We note that equation (15) is equivalent to equation (12) if  $c_\lambda$  in equation (12) is allowed to incorporate a factor proportional to the square root of  $R$  (an invariant).

We show in Figure 1 that the primary coefficient,  $c_\lambda$ , is inversely proportional to  $B^2$  for the experimental data of Sirivat and Warhaft (1983) for homogeneous turbulence with a constant temperature gradient. We also expect that  $c_\lambda$  should have a dependence on  $A$  similar to that proposed for  $c_\mu$ . Therefore, we propose the following form for the primary coefficient to allow it to vary as a function of  $A$  and  $B$ , representing the dynamic and thermal equilibrium ratios, respectively:

$$c_\lambda = \frac{1}{c_A A + c_B B^2} \quad (16)$$

From the data of Sirivat and Warhaft (1983), where  $A = 0$ , we determine  $c_B = 0.77$ . In order to determine  $c_A$ , we apply constant-stress and constant-flux assumptions, along with dynamic and thermal equilibrium, in the velocity and temperature log-law region of a boundary layer. In this region,  $A = 3.3$ ,  $B = 2.2$ , and  $c_\lambda = 0.2$ , which determines  $c_A = 0.38$ .

The constants  $c_{\tau\theta 1}$ ,  $c_{\tau\theta 2}$ ,  $c_{\tau\theta 3}$ , and  $c_{\tau\theta 4}$  remain to be determined. We shall exploit some experimental observations about the behavior of the time scale ratio,  $R$ , using a method similar to that of Jones and Musonge (1988). First we consider the decaying homogeneous turbulence experiment of Warhaft and Lumley (1978), where  $R$  remained constant. We construct a transport equation for  $R$  from those for  $\tau$  and  $\tau_\theta$ :

$$U \frac{dR}{dx} = U \left[ \frac{1}{\tau} \frac{d\tau_\theta}{dx} - \frac{\tau_\theta}{\tau^2} \frac{d\tau}{dx} \right] = c_{\tau\theta 3} \frac{\tau_\theta}{\tau^2} - c_{\tau\theta 4} \frac{1}{\tau} - c_{\tau 2} \frac{\tau_\theta}{\tau^2} \quad (17)$$

Equating the above to zero determines  $c_{\tau\theta 4} = 0$  and  $c_{\tau\theta 3} = c_{\tau 2} = 0.8$ .

Next, we consider the experimental data of Sirivat and Warhaft (1983) for homogeneous shear flows with constant temperature gradients. Here, the time scale ratio,  $R$ , while not constant, appeared to approach a constant value downstream. We again construct a transport equation for  $R$ :

$$\begin{aligned} U \frac{dR}{dx} &= U \left[ \frac{1}{\tau} \frac{d\tau_\theta}{dx} - \frac{\tau_\theta}{\tau^2} \frac{d\tau}{dx} \right] \\ &= c_{\tau\theta 1} \frac{\tau_\theta}{\tau k_\theta} P_k + c_{\tau\theta 3} \frac{\tau_\theta}{\tau^2} - c_{\tau 2} \frac{\tau_\theta}{\tau^2} \end{aligned} \quad (18)$$

Equating the above to zero with  $c_{\tau\theta 3} = c_{\tau 2}$  determines  $c_{\tau\theta 1} = 0$ .

Finally, we consider the experiment of Tavoularis and Corrsin (1981) for a homogeneous shear flow with constant velocity gradient and constant temperature gradient. Once again, the time scale ratio appeared to remain constant through the entire experimental domain. We again construct a transport equation for  $R$ :

$$\begin{aligned} U \frac{dR}{dx} &= U \left[ \frac{1}{\tau} \frac{d\tau_\theta}{dx} - \frac{\tau_\theta}{\tau^2} \frac{d\tau}{dx} \right] \\ &= c_{\tau\theta 2} \frac{\tau_\theta}{\tau k} P_k + c_{\tau\theta 3} \frac{\tau_\theta}{\tau^2} + c_{\tau 1} \frac{\tau_\theta}{\tau k} P_k - c_{\tau 2} \frac{\tau_\theta}{\tau^2} \end{aligned} \quad (19)$$

Equating the above to zero with  $c_{\tau\theta 3} = c_{\tau 2}$  determines  $c_{\tau\theta 2} = -c_{\tau 1} = -0.44$ . We can now write equation (9) as:

$$U \frac{d\tau_\theta}{dx} = -c_{\tau 1} \frac{\tau_\theta}{k} P_k + c_{\tau 2} \frac{\tau_\theta}{\tau} \quad (20)$$

We now have a complete thermal turbulence model with only two constants which are determined to be equal to their counterparts in the dynamic turbulence model. These constants are related to the well-tested standard constants for the  $\epsilon$  transport equation,  $c_{\epsilon 1} = 1.44$ , and  $c_{\epsilon 2} = 1.8$ . In contrast, the YNT and SSZ models each contain four constants to be determined. The published values for all the constants used in the YNT and SSZ models are shown in Table 1.

## MODEL VALIDATION

We consider three classic sets of experimental data (Warhaft and Lumley, 1978; Sirivat and Warhaft, 1983; and Tavoularis and Corrsin, 1981) to validate our new model for homogeneous shear flows. While these are the same data used to evaluate the thermal constants in our model, we did not "tune" any of these constants to

match the data; rather, we used observations about the evolution of the variable time scale ratio, as shown by the data, to evaluate these constants in terms of the well-established dynamic constants used in standard  $k$ - $\epsilon$  models.

Various second-moment models (for example: Shih and Lumley, 1986; Jones and Musonge, 1988; Shikazono and Kasagi, 1993) have successfully predicted these types of homogeneous shear flows. While we cannot hope to compete with a second-moment model in predicting these flows, we present our predictions in an attempt to systematically validate our new model.

We also compare the predictions of our model against the predictions obtained from the YNT and SSZ models, although it might be argued that this is an unfair comparison, since models developed specifically for wall-bounded shear flows can require modification of their constants when used to predict free-shear flows or homogeneous shear flows. However, we present these comparisons in an attempt to establish a more universally-applicable model at this level.

All four transport equations for each model, represented by ordinary differential equations for homogeneous shear flows, were integrated using a standard four-step Runge-Kutta method adapted from White (1974). The integration steps were sufficiently small to compute results identical to known polynomial and exponential solutions of similar equations. Furthermore, computed results for the actual model equations using smaller integration steps were indistinguishable from those presented herein.

We first consider the simplest case of decaying homogeneous dynamic and thermal turbulence (Warhaft and Lumley, 1978). The dynamic turbulence was generated by a uniform biplane grid, while the thermal turbulence was generated by a "mandoline" array of parallel heated wires. The experiment was conducted at a Reynolds number of 10,000 based on a mean velocity of 6.5 m/s and a grid spacing,  $M$ , of 0.0254 m. Four different initial time scale ratios were imposed by varying the downstream location of the mandoline, the mandoline wire spacing, and the electrical current applied to the mandoline: Case I,  $R = 1.04$ ; Case II,  $R = 0.73$ ; Case III,  $R = 0.65$ ; and Case IV,  $R = 0.42$ . The dynamic turbulence field was identical for each of these four cases. All dependent variables are normalized by their initial values, while the independent variable,  $x$ , is normalized by the grid spacing,  $M$ .

The dynamic turbulence results are shown in figure 2. Both  $k^*$  and  $\epsilon^*$  decay at a uniform exponential rate, while  $\tau^*$  grows at an exponential rate. The predictions of all three models are consistent with the experimental data, as expected, since the constant  $c_{\tau 2}$  was originally evaluated for this type of flow.

The thermal turbulence results are shown in figure 3, with parts (a)-(d) corresponding to the four values for  $R$  imposed in the experiment. For all four cases, our new model appears to match the data more closely than the other models, although they also predict an exponential decay for  $k_\theta^*$  and  $\epsilon_\theta^*$ , and an exponential growth for  $\tau_\theta^*$ , as expected. The predictions of the SSZ model appear slightly worse than those of the YNT model.

We next consider homogeneous turbulence with a constant mean temperature gradient, but zero mean velocity gradient (Sirivat and Warhaft, 1983; Shih and Lumley, 1986). The dynamic turbulence was again generated by a uniform biplane grid, while the thermal turbulence was generated by either a "mandoline" array of

parallel heated wires or a "toaster" array of heated ribbons. The mean temperature gradient was maintained by differentially heating the individual wires or ribbons. The experiments were conducted at two Reynolds numbers, based on mean velocity and grid spacing; various combinations of heater configurations and applied electrical current were then used to generate different values of temperature gradient and initial time scale ratio. Table 2 summarizes the seven test cases used by Shih and Lumley (1986), and selected for this work. The dependent variables are normalized by derived initial scales for each case, while the independent variable,  $x$ , is again normalized by the grid spacing,  $M$ .

The dynamic turbulence results are shown in figure 4(a) and (b) for the high and low Reynolds number cases. The predictions of all three models are consistent with the experimental data for both cases, and are very similar to those shown in figure 2, as expected.

The thermal turbulence results are shown in figures 5 through 11, corresponding to each of the seven test cases. Parts (a), (b), and (c) of each figure show the downstream evolution of  $k_\theta^*$ ,  $\epsilon_\theta^*$ , and  $\tau_\theta^*$ ; the time scale ratio,  $R$ ; and the turbulent heat flux,  $\langle v\theta \rangle^*$ , respectively. An additional prediction for  $\langle v\theta \rangle^*$  from a standard  $k$ - $\epsilon$  model with constant  $Pr_t = 0.9$  is shown as a dotted-dashed line in part (c) of each figure.

The predictions of our new model show the best agreement with the data for cases 1, 2, and 3, shown in figures 5, 6, and 7, respectively. The time scale ratio is adequately predicted as a constant by our new model for all cases except case 7, shown in figure 11, which exhibits an initial decay in  $k_\theta^*$  and  $R$  that would be impossible to model with any gradient-diffusion-based model for a constant mean temperature gradient. The turbulent heat flux predictions exhibit the proper downstream decay in figures 5(c), 6(c), and 7(c). The new model predictions for cases 4, 5, and 6, shown in figures 8, 9, and 10, respectively, show poorer agreement with the data, especially for the turbulent heat flux in part (c) of each figure.

In all cases, the YNT and SSZ model predictions are in generally worse agreement with the experimental data than the predictions of our new model. The YNT model typically overpredicts  $k_\theta^*$  and  $\langle v\theta \rangle^*$ , while the SSZ model typically underpredicts them; both models overpredict  $\tau_\theta^*$ . These effects can be traced to the nature of the constitutive equations used by each model for computing the turbulent heat flux. The YNT model computes  $\langle v\theta \rangle^*$ , and therefore, production of  $k_\theta^*$ , as proportional to  $(2R)^2$ , while the SSZ model computes it as proportional to  $(2R)^{0.5}$ . As the computed value of  $R$  departs from its generally-assumed equilibrium value of 0.5, the YNT and SSZ model predictions exhibit markedly different behavior. For case 6, shown in figure 10,  $R$  is very close to 0.5, and the YNT and SSZ model predictions are very similar. For all cases, the prediction of  $\langle v\theta \rangle^*$  using the standard  $k$ - $\epsilon$  model with  $Pr_t = 0.9$  is roughly constant, as we would expect, and clearly inadequate.

We finally consider homogeneous turbulence with both mean temperature gradient and mean velocity gradient (Tavoularis and Corrsin, 1981). The mean velocity gradient ( $dU/dy = 46.8 \text{ s}^{-1}$ ) was generated by a series of ten parallel channels with individual throttle screens to vary the mean velocity. The dynamic and thermal turbulence was generated by electrically-heated rods placed in each channel. The mean temperature gradient ( $d\theta/dy = 9.5 \text{ K/m}$ )

was maintained by differential heating of the rods. The dependent variables are normalized by derived initial scales, while the independent variable,  $x$ , is normalized by the total channel height,  $h$ .

The dynamic turbulence predictions are shown in figure 12. The new model predictions for  $k^*$ ,  $\epsilon^*$ , and  $\tau^*$ , while not in perfect agreement with the data, do show the proper quadratic behavior for  $k^*$  and  $\epsilon^*$ , while  $\tau^*$  decays slightly, rather than remaining constant. The new model prediction for  $\langle uv \rangle^*$  also exhibits the proper behavior, disallowing a slight overprediction. The YNT and SSZ model predictions are clearly inferior.

The thermal turbulence predictions are shown in figure 13. The new model predictions for  $k_\theta^*$ ,  $\epsilon_\theta^*$ , and  $\tau_\theta^*$  match the experimental data very well, as does the prediction for  $R$ . The new model slightly underpredicts  $\langle v\theta \rangle^*$ , although it clearly shows the proper trend. The YNT and SSZ model predictions are clearly inferior, except for the time scale ratio. The prediction of  $\langle v\theta \rangle^*$  using the standard  $k$ - $\epsilon$  model with  $Pr_t = 0.9$  is also markedly inferior.

## CONCLUSIONS

A new turbulence model, based upon dynamic and thermal turbulent time scale transport equations, was developed and applied to homogeneous shear flows with constant velocity and temperature gradients. The new model comprised transport equations for  $k$ , the turbulent kinetic energy;  $\tau$ , the dynamic time scale;  $k_\theta$ , the fluctuating temperature variance; and  $\tau_\theta$ , the thermal time scale. It was proposed to offer conceptually parallel modelling of the dynamic and thermal turbulence at the two-equation level, and to eliminate the customary prescription of an empirical turbulent Prandtl number,  $Pr_t$ , thus permitting a more generalized prediction capability for turbulent heat transfer in complex flows and geometries.

The dynamic and thermal time scales were chosen as dependent variables to eventually exploit their potential for simpler wall boundary conditions than those used for the traditional choice of the dissipation rates as dependent variables. The new model also incorporated constitutive relations, based upon invariant theory, that allowed the effects of non-equilibrium in the dynamic and thermal turbulence to modify the primary coefficients for the turbulent stress and heat flux.

Predictions of the new model, along with those from the YNT and SSZ models, were compared with experimental data for decaying homogeneous dynamic and thermal turbulence, homogeneous turbulence with constant temperature gradient, and homogeneous turbulence with constant temperature gradient and constant velocity gradient. In general, the new model showed improvement in agreement with the data, although in several cases it was no better than the other models.

The homogeneous shear flows considered in this work represented canonical cases that any universal dynamic and thermal turbulence model should be able to predict. Our new model showed some ability to offer better predictions than the other models for a limited parametric range of constant time scale ratio, constant mean temperature gradient, and constant mean velocity gradient for these flows. Further work will be required to evaluate the new model for the eventual goal of predicting wall-bounded shear flows, where the variation of the time scale ratio, dynamic equilib-

rium, and thermal equilibrium may affect the turbulence differently than for these homogeneous shear flows.

## ACKNOWLEDGMENT

The authors thank Dr. Aamir Shabbir, of the Institute for Computational Mechanics in Propulsion, Center for Modelling of Turbulence and Transition, NASA Lewis Research Center, for helpful discussions regarding this work

## REFERENCES

- Antonia, R. A., and Kim, J., 1991, "Turbulent Prandtl Number in the Near-Wall Region of a Turbulent Channel Flow," *International Journal of Heat and Mass Transfer*, Vol. 34, No. 7, pp. 1905-1908.
- Bagheri, N., Strataridakis, C. J., and White, B. R., 1992, "Measurements of Turbulent Boundary Layer Prandtl Numbers and Space-Time Temperature Correlations," *AIAA Journal*, Vol. 30, No. 1, pp. 35-42.
- Beguier, C., Dekeyser, I., and Launder, B. E., 1978, "Ratio of Scalar and Velocity Dissipation Time Scales in Shear Flow Turbulence," *Physics of Fluids*, Vol. 21, No. 3, pp. 307-310.
- Jones, W. P., and Musonge, P., 1988, "Closure of the Reynolds Stress and Scalar Flux Equations," *Physics of Fluids*, Vol. 31, No. 12, pp. 3589-3604.
- Lai, Y. G., and So, R. M. C., 1990, "Near-Wall Modelling of Turbulent Heat Fluxes," *International Journal of Heat and Mass Transfer*, Vol. 33, No. 7, pp. 1429-1440.
- Nagano, Y., and Kim, C., 1988, "A Two-Equation Model for Heat Transport in Wall Turbulent Shear Flows," *ASME Journal of Heat Transfer*, Vol. 110, pp. 583-589.
- Newman, G. R., Launder, B. E., and Lumley, J. L., 1981, "Modelling the Behaviour of Homogeneous Scalar Turbulence," *Journal of Fluid Mechanics*, Vol. 111, pp. 217-232.
- Reynolds, A. J., 1975, "The Prediction of Turbulent Prandtl and Schmidt Numbers," *International Journal of Heat and Mass Transfer*, Vol. 18, pp. 1055-1069.
- Shabbir, A., 1994, "Modeling of Homogeneous Scalar Turbulence," *Center for Modeling of Turbulence and Transition Research Briefs - 1993*, NASA TM-106383, pp. 67-79.
- Shih, T.-H., and Lumley, J. L., 1986, "Influence of Timescale Ratio on Scalar Flux Relaxation: Modelling Sirivat & Warhaft's Homogeneous Passive Scalar Fluctuations," *Journal of Fluid Mechanics*, Vol. 162, pp. 211-222.
- Shih, T.-H., and Lumley, J. L., 1993, "Remarks on Turbulent Constitutive Relations," NASA TM-106116.
- Shih, T.-H., Zhu, J., and Lumley, J. L., 1993, "A Realizable Reynolds Stress Algebraic Equation Model," NASA TM-105993.
- Shikazono, N., and Kasagi, N., 1993, "Modeling Prandtl Number Influence on Scalar Transport in Isotropic and Sheared Turbulence," *Ninth Symposium on Turbulent Shear Flows*, pp. 18-3-1 - 18-3-6.
- Sirivat, A., and Warhaft, Z., 1983, "The Effect of a Passive Cross-Stream Temperature Gradient on the Evolution of Temperature Variance and Heat Flux in Grid Turbulence," *Journal of Fluid Mechanics*, Vol. 128, pp. 323-346.

Sommer, T. P., So, R. M. C., and Zhang, H. S., 1993a, "On the Assumption of Vanishing Temperature Fluctuations at the Wall for Heat Transfer Modelling," AIAA 93-0088.

Sommer, T. P., So, R. M. C., and Zhang, H. S., 1993b, "Near-Wall Variable-Prandtl-Number Turbulence Model for Compressible Flows," *AIAA Journal*, Vol. 31, No. 1, pp. 27-35.

Speziale, C. G., Abid, R., and Anderson, E. C., 1992, "Critical Evaluation of Two-Equation Models for Near-Wall Turbulence," *AIAA Journal*, Vol. 30, No. 2, pp. 324-331.

Tavoularis, S., and Corrsin, S., 1981, "Experiments in Nearly Homogeneous Turbulent Shear Flow with a Uniform Mean Temperature Gradient, Part 1," *Journal of Fluid Mechanics*, Vol. 104, pp. 311-347.

Warhaft, Z., and Lumley, J. L., 1978, "An Experimental Study of the Decay of Temperature Fluctuations in Grid-Generated Turbulence," *Journal of Fluid Mechanics*, Vol. 88, pp. 659-684.

White, F. M., 1974, "Appendix C: A Runge-Kutta Subroutine for  $N$  Simultaneous Differential Equations," *Viscous Fluid Flow*, McGraw-Hill, Inc., pp. 675-678.

Youssef, M. S., Nagano, Y., and Tagawa, M., 1992, "A Two-Equation Heat Transfer Model for Predicting Turbulent Thermal Fields Under Arbitrary Wall Thermal Conditions," *International Journal of Heat and Mass Transfer*, Vol. 35, No. 11, pp. 3095-3104.

TABLE 1: SUMMARY OF MODEL CONSTANTS

Constant	YNT Model	SSZ Model
$c_\mu$	0.09	0.096
$c_{\epsilon 1}$	1.45	1.50
$c_{\epsilon 2}$	1.90	1.83
$c_\lambda$	0.10	0.11
$c_1$	0.85	0.90
$c_2$	0.64	0.72
$c_3$	1.00	1.10
$c_4$	0.90	0.80



TABLE 2: SUMMARY OF CASES FOR SIRIVAT AND WARHAFT EXPERIMENT

Case	$Re_M$	$d\Theta/dy$	$R_{initial}$
1	9545	10.3	0.547
2	9545	3.68	0.610
3	9545	4.48	0.612
4	5150	1.81	0.750
5	5150	8.10	0.772
6	5150	2.24	0.459
7	5150	1.78	0.676

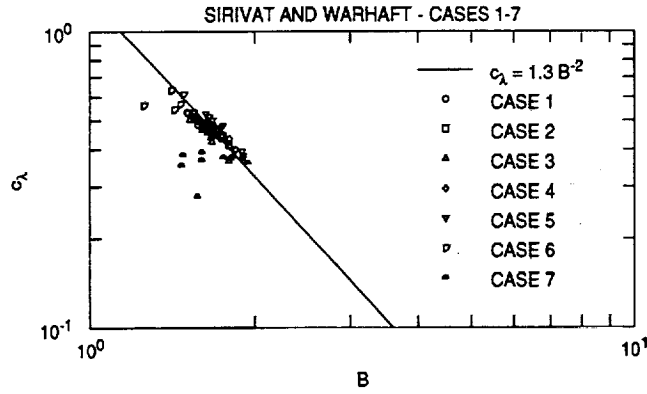


FIGURE 1: DEPENDENCE OF PRIMARY COEFFICIENT FOR TURBULENT HEAT FLUX

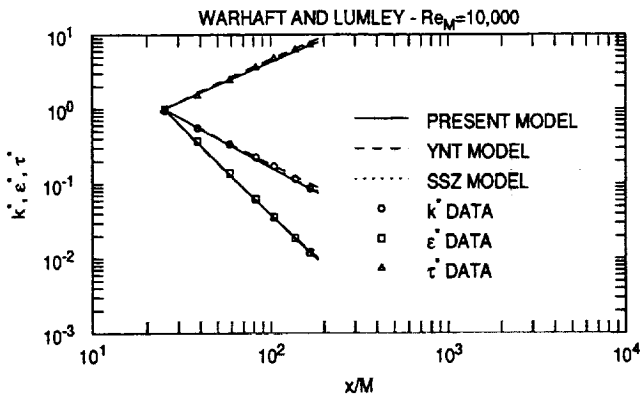


FIGURE 2: DYNAMIC TURBULENCE PREDICTIONS FOR WARHAFT AND LUMLEY EXPERIMENT

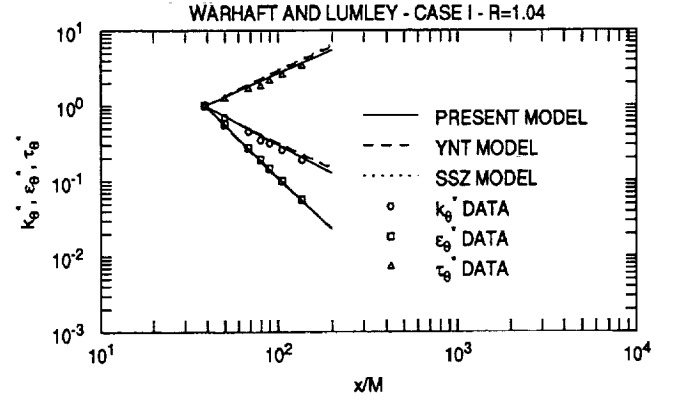


FIGURE 3(a): THERMAL TURBULENCE PREDICTIONS FOR WARHAFT AND LUMLEY CASE I

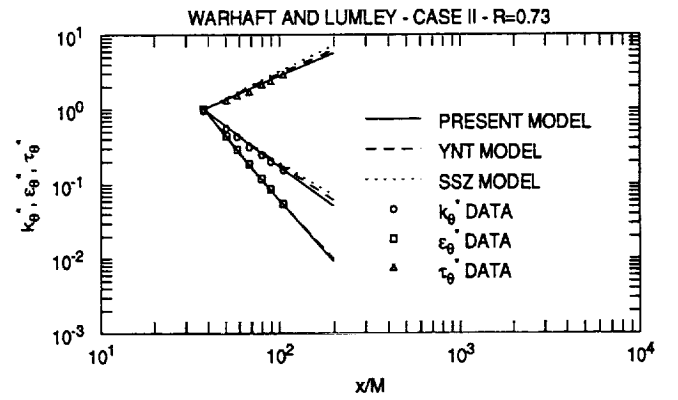


FIGURE 3(b): THERMAL TURBULENCE PREDICTIONS FOR WARHAFT AND LUMLEY CASE II

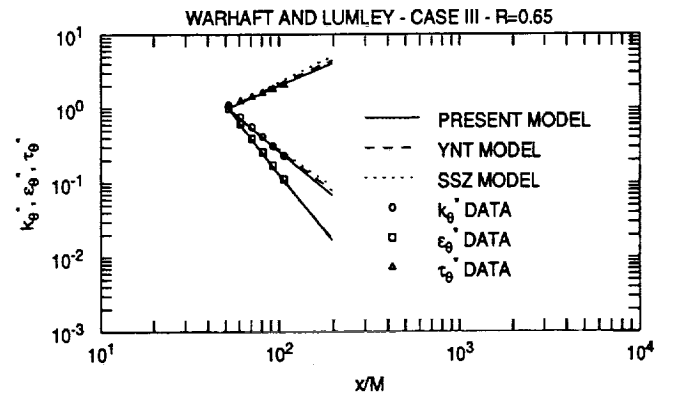


FIGURE 3(c): THERMAL TURBULENCE PREDICTIONS FOR WARHAFT AND LUMLEY CASE III

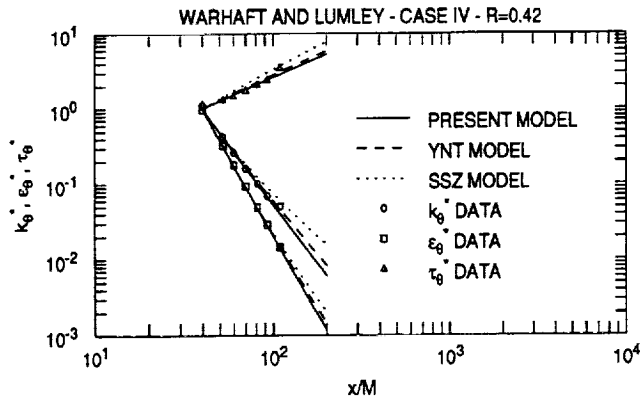


FIGURE 3(d): THERMAL TURBULENCE PREDICTIONS FOR WARHAFT AND LUMLEY CASE IV

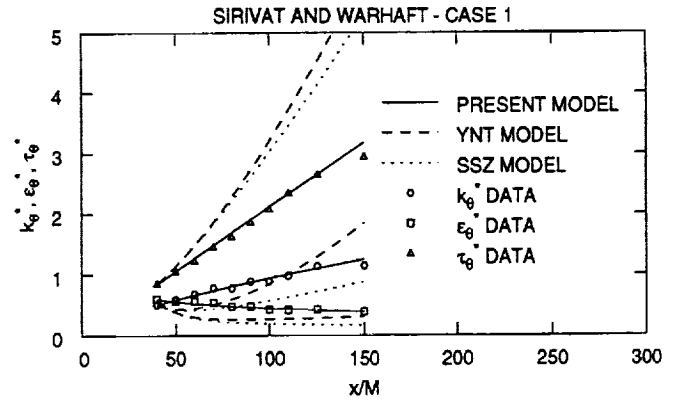


FIGURE 5(a): THERMAL TURBULENCE PREDICTIONS FOR SIRIVAT AND WARHAFT CASE 1

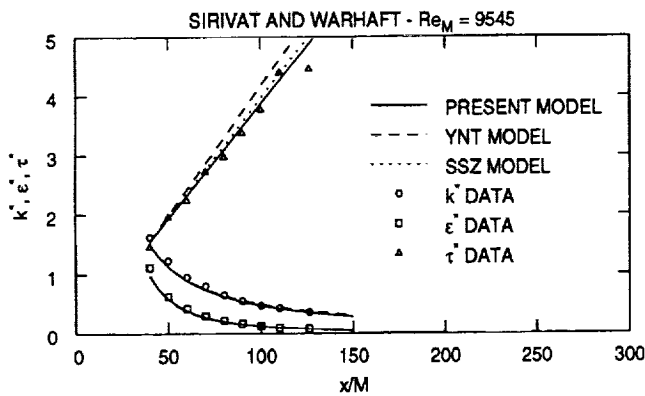


FIGURE 4(a): DYNAMIC TURBULENCE PREDICTIONS FOR SIRIVAT AND WARHAFT EXPERIMENT

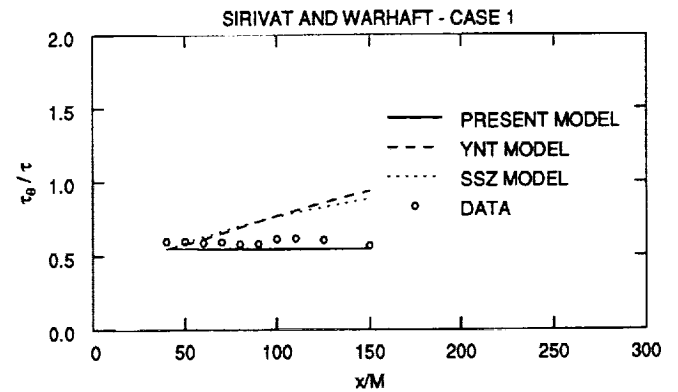


FIGURE 5(b): TIME SCALE RATIO PREDICTIONS FOR SIRIVAT AND WARHAFT CASE 1

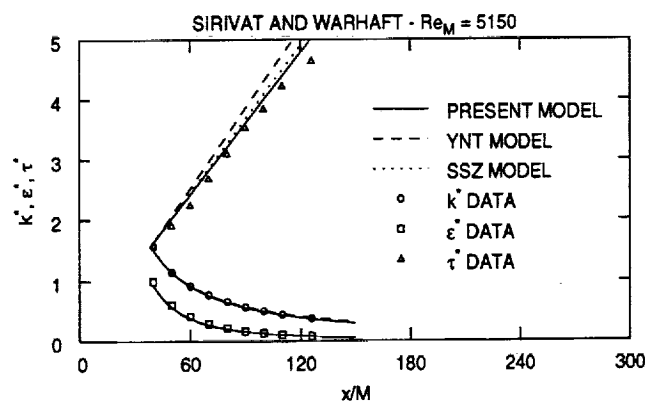


FIGURE 4(b): DYNAMIC TURBULENCE PREDICTIONS FOR SIRIVAT AND WARHAFT EXPERIMENT

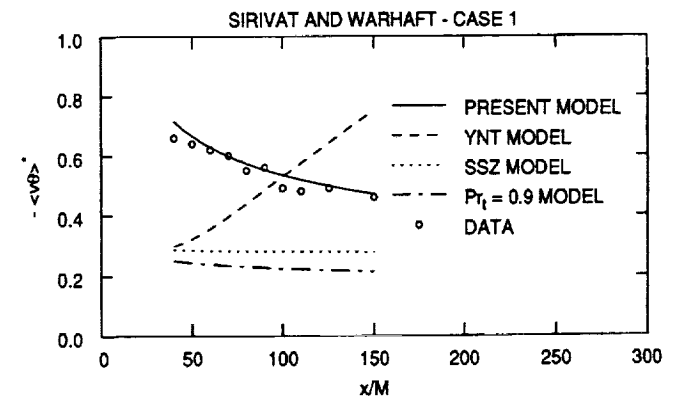


FIGURE 5(c): TURBULENT HEAT FLUX PREDICTIONS FOR SIRIVAT AND WARHAFT CASE 1

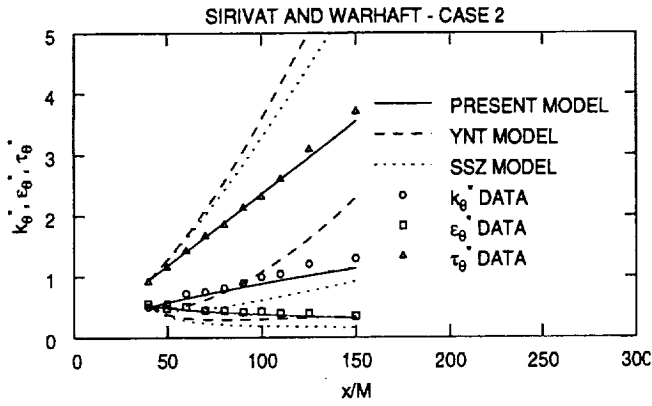


FIGURE 6(a): THERMAL TURBULENCE PREDICTIONS FOR SIRIVAT AND WARHAFT CASE 2

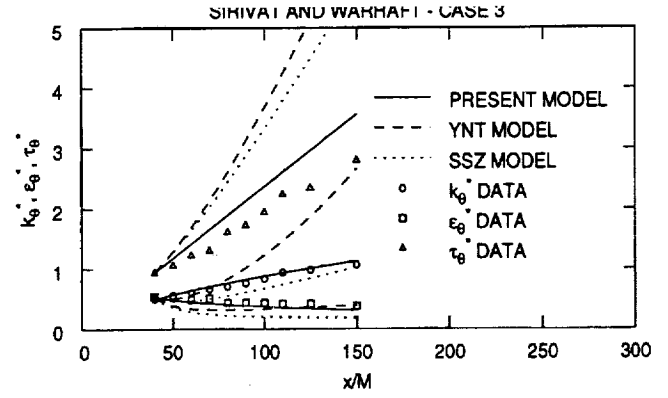


FIGURE 7(a): THERMAL TURBULENCE PREDICTIONS FOR SIRIVAT AND WARHAFT CASE 3

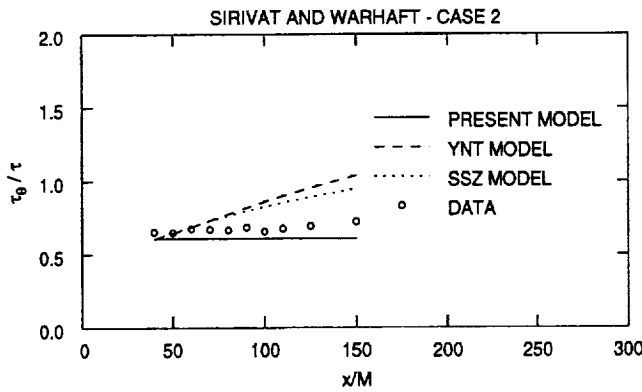


FIGURE 6(b): TIME SCALE RATIO PREDICTIONS FOR SIRIVAT AND WARHAFT CASE 2

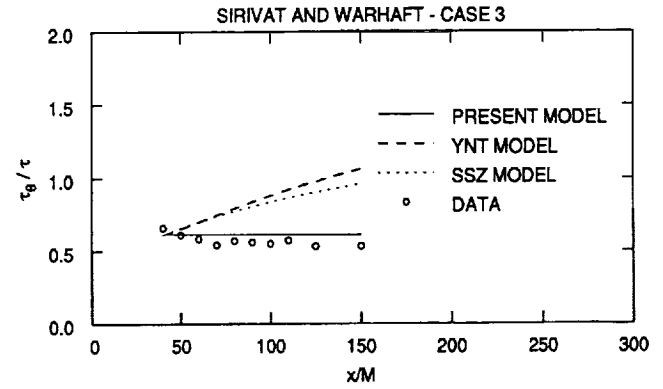


FIGURE 7(b): TIME SCALE RATIO PREDICTIONS FOR SIRIVAT AND WARHAFT CASE 3

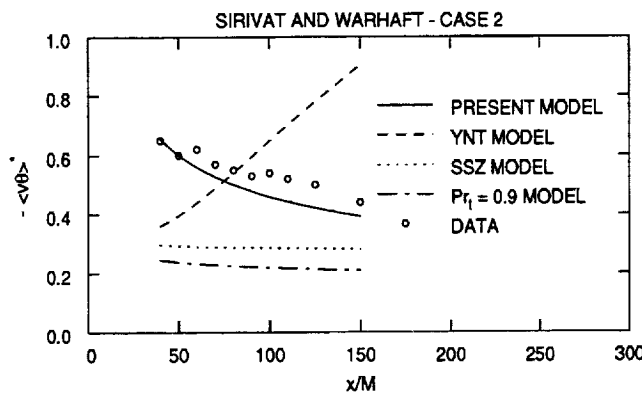


FIGURE 6(c): TURBULENT HEAT FLUX PREDICTIONS FOR SIRIVAT AND WARHAFT CASE 2

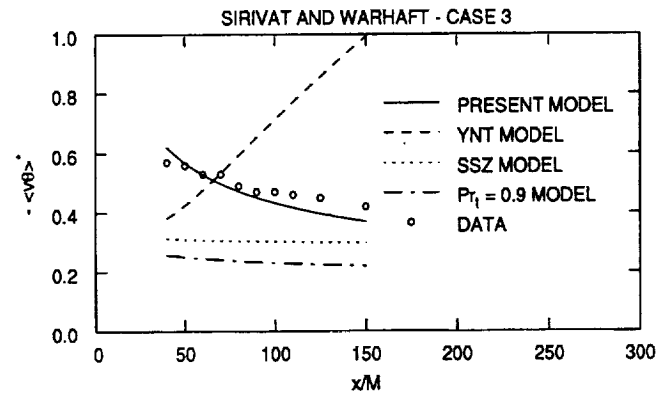


FIGURE 7(c): TURBULENT HEAT FLUX PREDICTIONS FOR SIRIVAT AND WARHAFT CASE 3

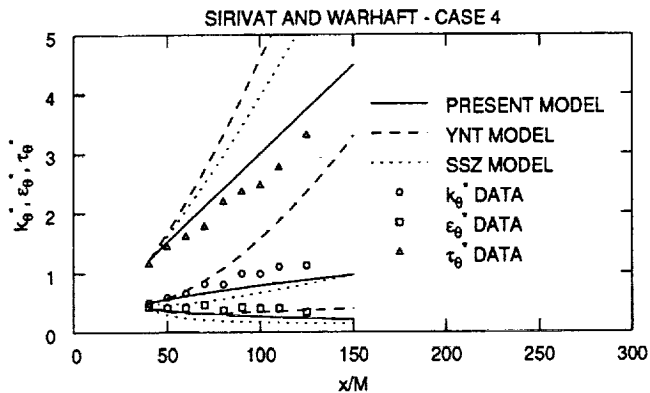


FIGURE 8(a): THERMAL TURBULENCE PREDICTIONS FOR SIRIVAT AND WARHAFT CASE 4

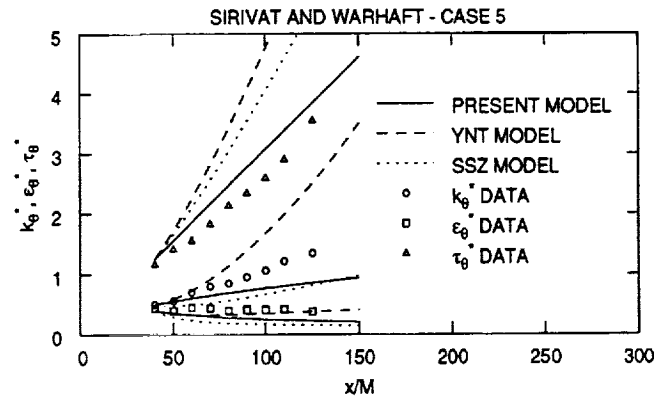


FIGURE 9(a): THERMAL TURBULENCE PREDICTIONS FOR SIRIVAT AND WARHAFT CASE 5

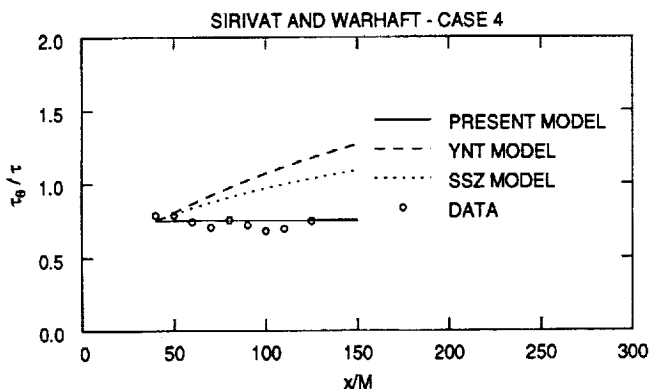


FIGURE 8(b): TIME SCALE RATIO PREDICTIONS FOR SIRIVAT AND WARHAFT CASE 4

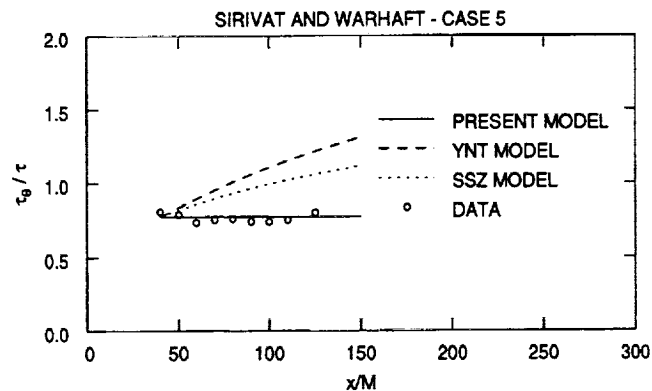


FIGURE 9(b): TIME SCALE RATIO PREDICTIONS FOR SIRIVAT AND WARHAFT CASE 5

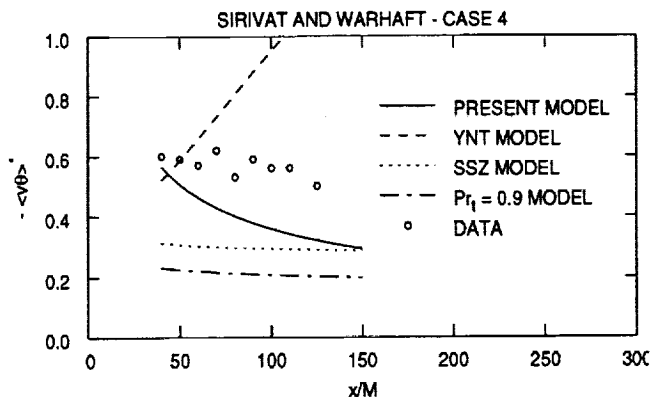


FIGURE 8(c): TURBULENT HEAT FLUX PREDICTIONS FOR SIRIVAT AND WARHAFT CASE 4

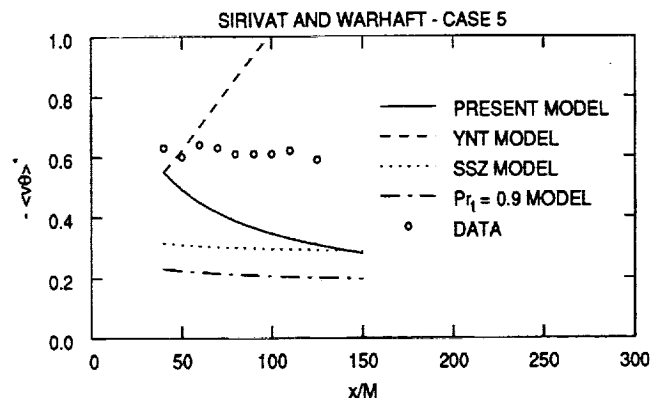


FIGURE 9(c): TURBULENT HEAT FLUX PREDICTIONS FOR SIRIVAT AND WARHAFT CASE 5

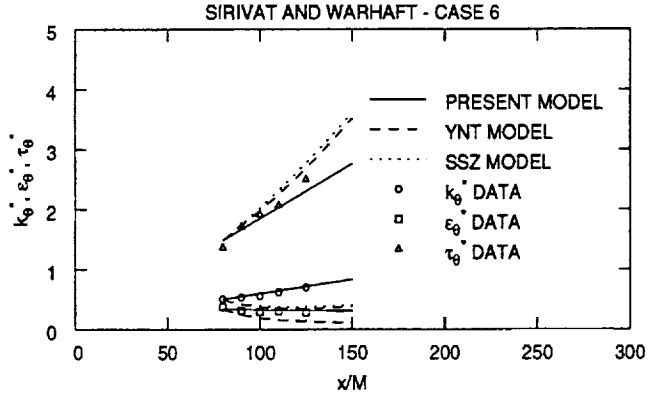


FIGURE 10(a): THERMAL TURBULENCE PREDICTIONS FOR SIRIVAT AND WARHAFT CASE 6

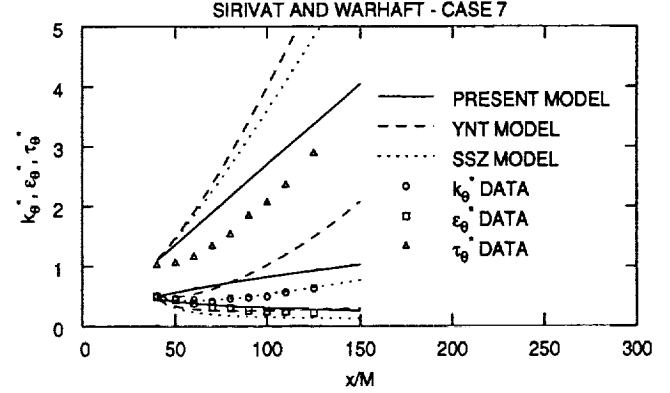


FIGURE 11(a): THERMAL TURBULENCE PREDICTIONS FOR SIRIVAT AND WARHAFT CASE 7

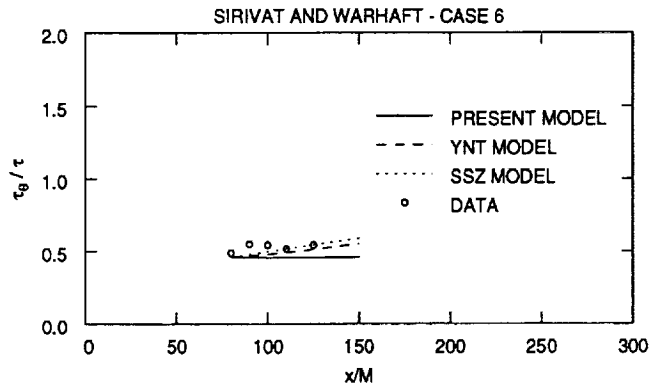


FIGURE 10(b): TIME SCALE RATIO PREDICTIONS FOR SIRIVAT AND WARHAFT CASE 6

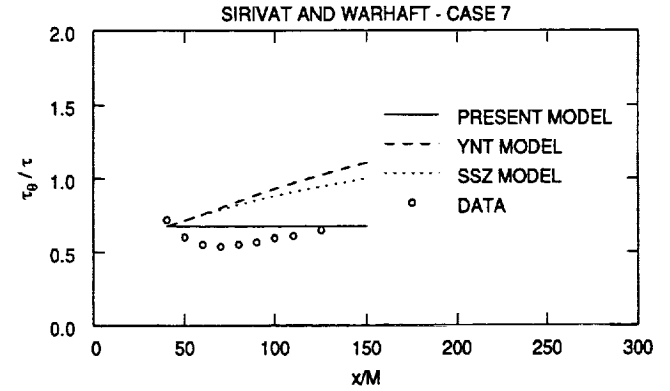


FIGURE 11(b): TIME SCALE RATIO PREDICTIONS FOR SIRIVAT AND WARHAFT CASE 7

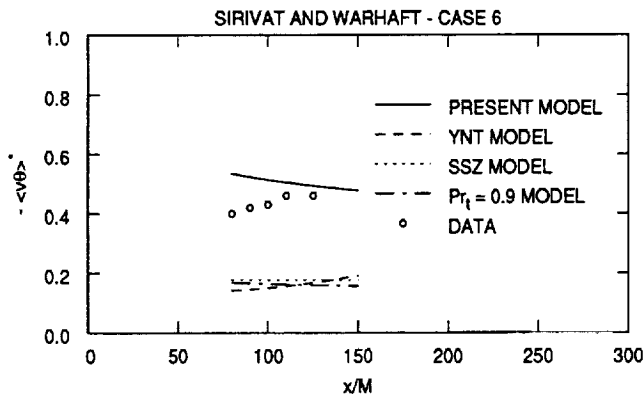


FIGURE 10(c): TURBULENT HEAT FLUX PREDICTIONS FOR SIRIVAT AND WARHAFT CASE 6

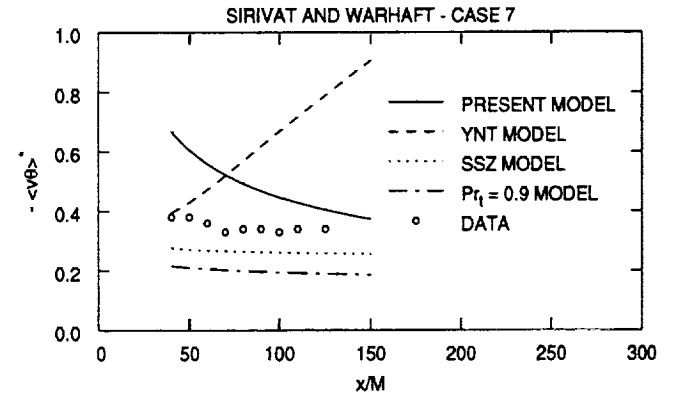


FIGURE 11(c): TURBULENT HEAT FLUX PREDICTIONS FOR SIRIVAT AND WARHAFT CASE 7

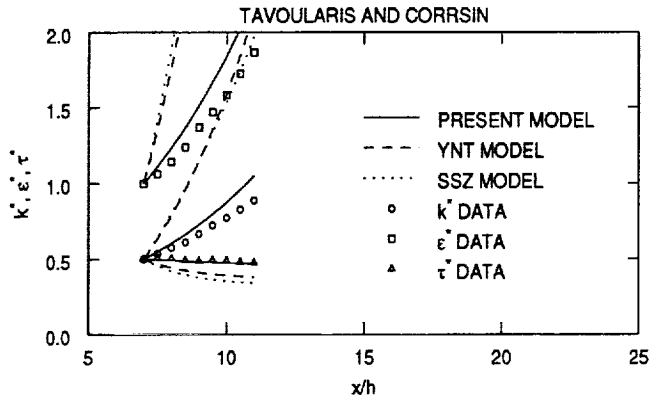


FIGURE 12(a): DYNAMIC TURBULENCE PREDICTIONS FOR TAVOULARIS AND CORRSIN EXPERIMENT

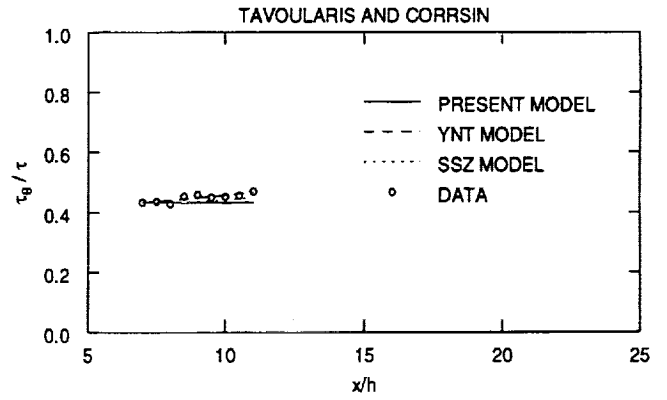


FIGURE 13(b): TIME SCALE RATIO PREDICTIONS FOR TAVOULARIS AND CORRSIN EXPERIMENT

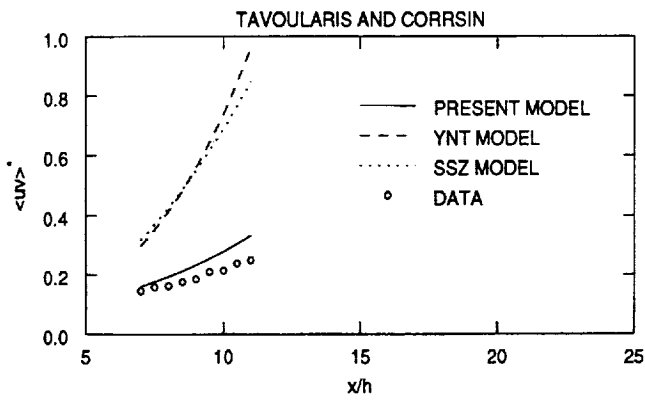


FIGURE 12(b): TURBULENT STRESS PREDICTIONS FOR TAVOULARIS AND CORRSIN EXPERIMENT

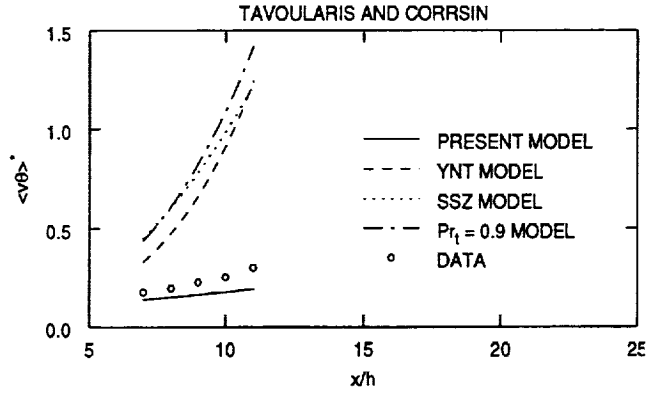


FIGURE 13(c): TURBULENT HEAT FLUX PREDICTIONS FOR TAVOULARIS AND CORRSIN EXPERIMENT

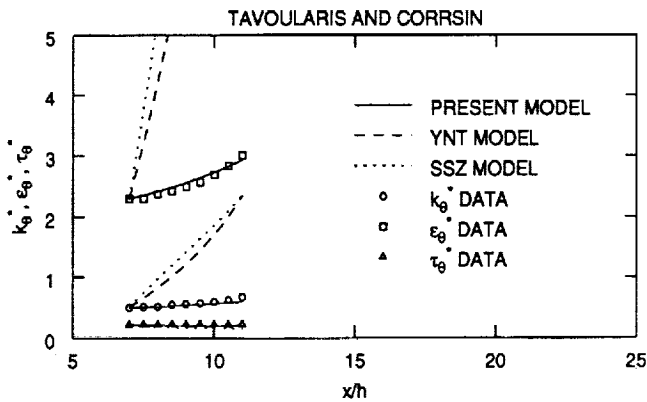


FIGURE 13(a): THERMAL TURBULENCE PREDICTIONS FOR TAVOULARIS AND CORRSIN EXPERIMENT



REPORT DOCUMENTATION PAGE			Form Approved OMB No. 0704-0188	
Public reporting burden for this collection of information is estimated to average 1 hour per response, including the time for reviewing instructions, searching existing data sources, gathering and maintaining the data needed, and completing and reviewing the collection of information. Send comments regarding this burden estimate or any other aspect of this collection of information, including suggestions for reducing this burden, to Washington Headquarters Services, Directorate for Information Operations and Reports, 1215 Jefferson Davis Highway, Suite 1204, Arlington, VA 22202-4302, and to the Office of Management and Budget, Paperwork Reduction Project (0704-0188), Washington, DC 20503.				
1. AGENCY USE ONLY (Leave blank)	2. REPORT DATE June 1994	3. REPORT TYPE AND DATES COVERED Technical Memorandum		
4. TITLE AND SUBTITLE  Dynamic and Thermal Turbulent Time Scale Modelling for Homogeneous Shear Flows		5. FUNDING NUMBERS  WU-505-62-52		
6. AUTHOR(S)  John R. Schwab and Budugur Lakshminarayana				
7. PERFORMING ORGANIZATION NAME(S) AND ADDRESS(ES)  National Aeronautics and Space Administration Lewis Research Center Cleveland, Ohio 44135-3191		8. PERFORMING ORGANIZATION REPORT NUMBER  E-8936		
9. SPONSORING/MONITORING AGENCY NAME(S) AND ADDRESS(ES)  National Aeronautics and Space Administration Washington, D.C. 20546-0001		10. SPONSORING/MONITORING AGENCY REPORT NUMBER  NASA TM-106635		
11. SUPPLEMENTARY NOTES Prepared for the Fluids Engineering Division Summer Meeting sponsored by the American Society for Mechanical Engineers, Lake Tahoe, Nevada, June 19-23, 1994. John R. Schwab, NASA Lewis Research Center, and Budugur Lakshminarayana, Pennsylvania State University, Department of Aerospace Engineering, University Park, Pennsylvania 16804. Responsible person, John R. Schwab, organization code 2640, (216) 433-8446.				
12a. DISTRIBUTION/AVAILABILITY STATEMENT  Unclassified - Unlimited Subject Category 34			12b. DISTRIBUTION CODE	
13. ABSTRACT (Maximum 200 words)  A new turbulence model, based upon dynamic and thermal turbulent time scale transport equations, is developed and applied to homogeneous shear flows with constant velocity and temperature gradients. The new model comprises transport equations for $k$ , the turbulent kinetic energy; $\tau$ , the dynamic time scale; $k_\theta$ , the fluctuating temperature variance; and $\tau_\theta$ , the thermal time scale. It offers conceptually parallel modelling of the dynamic and thermal turbulence at the two-equation level, and eliminates the customary prescription of an empirical turbulent Prandtl number, $Pr_t$ , thus permitting a more generalized prediction capability for turbulent heat transfer in complex flows and geometries. The new model also incorporates constitutive relations, based upon invariant theory, that allow the effects of non-equilibrium to modify the primary coefficients for the turbulent shear stress and heat flux. Predictions of the new model, along with those from two other similar models, are compared with experimental data for decaying homogeneous dynamic and thermal turbulence, homogeneous turbulence with constant temperature gradient, and homogenous turbulence with constant temperature gradient and constant velocity gradient. The new model offers improvement in agreement with the data for most cases considered in this work, although it was no better than the other models for several cases where all the models performed poorly.				
14. SUBJECT TERMS  Turbulence modeling			15. NUMBER OF PAGES 14	
			16. PRICE CODE A03	
17. SECURITY CLASSIFICATION OF REPORT Unclassified	18. SECURITY CLASSIFICATION OF THIS PAGE Unclassified	19. SECURITY CLASSIFICATION OF ABSTRACT Unclassified	20. LIMITATION OF ABSTRACT	